Pol. J. Environ. Stud. Vol. 33, No. 2 (2024), 1443-1453
DOI: *10.15244/pjoes/173437* ONLINE PUBLICATION DATE: 2023-11-27

Original Research

Concentrations, Sources, and Correlation Analysis of Polycyclic Aromatic Hydrocarbons in Atmospheric Particulate Matter and Organic Film from Shanghai, China

Yingpeng Yu[1]*, Min Liu[2, 3, 4], Feng Liang[1], Wenlei Niu[1], Xue Zhu[5], Jing Tao[5]

[1]Tourism Research Centre, Wuxi Institute of Technology, Wuxi, 214121, China
[2]Key Laboratory of Geographic Information Science, Ministry of Education, East China Normal University, Shanghai, 200241, China
[3]School of Geographic Sciences, East China Normal University, Shanghai, 200241, China
[4]Key Laboratory of Spatial-temporal Big Data Analysis and Application of Natural Resources in Megacities, Ministry of Natural Resources, Shanghai, 200241, China
[5]School of Foreign Language and Tourism, Wuxi Institute of Technology, Wuxi, 214121, China

Received: 23 August 2023
Accepted: 6 October 2023

Abstract

To understand the enrichment concentrations, compositional characteristics, and sources of polycyclic aromatic hydrocarbons (PAHs) in atmospheric particulate matter (PM) and organic film, $PM_{2.5}$, PM_{10}, and organic film on glass surfaces were collected from eight sampling sites in central urban, suburban, and rural Shanghai. Sixteen priority-controlled PAHs were investigated using gas chromatography-mass spectrometry, and mass concentrations, compositional differences, and pollution sources of PAHs in PM and organic film were analyzed. The results indicate that under good air conditions, 2.5-10 μm particles are relatively abundant in the atmosphere; during haze periods, PM is generally less than 2.5 μm. Furthermore, PAHs tend to adsorb on PM less than 2.5 μm. Except at Shengang (SG), 4-ring PAHs are particularly abundant in PM, while 2- and 3-ring PAHs are particularly abundant in organic film. The K_{FA} of low molecular weight PAHs is higher than the K_{OA}, indicating that these monomer PAHs have achieved dynamic equilibrium between the organic film and the atmosphere. Source identification results show that PAHs in PM and organic film are generated by vehicle exhaust, domestic exhaust gas, and ground dust.

Keywords: Shanghai; $PM_{2.5}$ and PM_{10}, organic film, polycyclic aromatic hydrocarbons, correlation analysis

*e-mail: yuyp@wxit.edu.cn

Introduction

Atmospheric particulate matter (PM) is considered a significant air pollutant that poses a threat to human health: it can cause cardiovascular disease, lung function damage, and increased cancer risk [1-4]. In recent years, a global continuous monitoring network for PM has been established, and relevant policies have been formulated to eliminate PM pollution [5]. Related studies have mainly focused on PM of sizes less than or equal to 2.5 μm ($PM_{2.5}$) or 10 μm (PM_{10}). The possible damage that can be caused by PM varies according to the PM's physical properties, chemical composition, and origin [6]. PAHs are products of incomplete combustion, and prolonged exposure to PAHs can lead to a range of cancer-related health problems [7, 8]. $PM_{2.5}$ and PM_{10} combined with PAHs can cause different health effects [9-13]. Currently, long-term and synchronous monitoring of $PM_{2.5}$- and PM_{10}-bound PAHs is very limited, especially in developing countries suffering from severe air pollution [1].

Impervious surface cover within urban environments alters the hydrology, energy distribution, and non-point source pollution load [14, 15]. Research has found that impervious surfaces can develop organic film 11-1000 nm thick and with an organic matter content of 5-40%. This organic film has a substantial impact on the migration and fate of organic pollutants in the surrounding environment [16]. A variety of persistent organic pollutants, including polycyclic aromatic hydrocarbons (PAHs), have been detected in organic film on glass surfaces [17]. In addition, organic film has the ability to respond quickly to changes in air pollution [18]. The film can record the air quality at the time of sampling and predict short-term changes in airborne organic pollutants [19, 20].

In 2022, $PM_{2.5}$ and PM_{10} were the primary airborne pollutants in 141 cities in China [21]. PAHs are carried by $PM_{2.5}$ into human alveoli and pose a substantial threat to human health [13]. Therefore, taking into consideration Shanghai's dominant wind direction and urban-rural gradient, this study selected representative sampling sites to measure and compare the component characteristics and pollution levels of PAHs in $PM_{2.5}$, PM_{10}, and organic film. The study also examined the distribution characteristics of PAHs in the organic film-atmosphere and analyzed the PAH sources in order to provide theoretical and data support for the study of multimedia urban PAHs.

Materials and Methods

Sample Collection

Using Zhongshan Park as the central sampling location, seven sampling sites were selected, including central urban (Zhongshan Park-ZSP), suburban (Tangqiao-TQ, Zhoupu-ZP, Huinan-HN, Jiuting-JT, and Songjiang University Town-SJUT), and rural (Shengang-SG) sites (Fig.1). In addition, samples of $PM_{2.5}$ and PM_{10} under haze (ECNU(H)) and non-haze (ECNU(NH)) weather conditions were collected at East China Normal University (ECNU). Two total suspended particulate (TSP) integrated samplers (Laoying 2050, Qingdao Laoying, China) were used to collect $PM_{2.5}$ and PM_{10} samples between 8:00 a.m. and 6:00 p.m. using the process developed by Wang et al. [22]. The sampling data

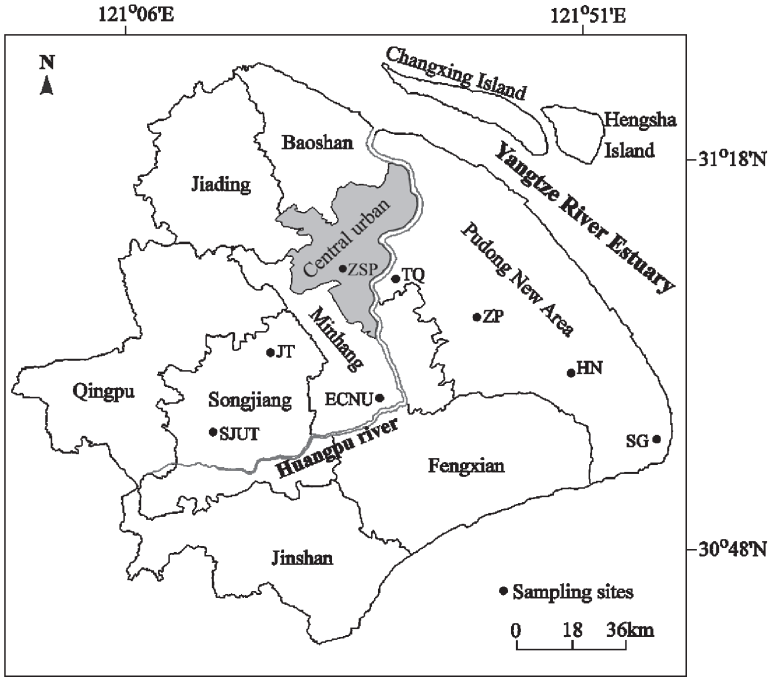

Fig. 1. Locations of atmospheric particulate matter and organic film sampling sites.

Table 1. Sampling data and meteorological parameters.

Sampling site	$PM_{2.5}$		PM_{10}		T(ºC)	W	WD	WS
	SV (L)	MC (mg/m^3)	SV (L)	MC (mg/m^3)				
ZSP	69265.0	12.27	68716.0	37.98	5-14	Sunny	Southwestern	3-4
JT	67445.3	9.79	67401.0	47.92	7-17	Cloudy	Southeastern	3-4
SJUT	70175.9	7.55	70054.8	58.53	3-10	Cloudy	Northwestern	5-6
TQ	69296.3	15.01	69529.7	54.08	4-13	Sunny	Northwestern	3-4
ZP	68578.0	15.75	68722.0	44.24	7-14	Sunny	Northwestern	3-4
HN	68650.0	12.53	68580.5	49.58	9-18	Cloudy	Northeastern	3-4
SG	69194.9	12.86	69274.3	89.50	9-17	Cloudy-sunny	Southwestern	3-4
ECNU(H)	82158.6	224.44	82172.1	248.99	8-13	Cloudy	Northwestern	3-4
ECNU(NH)	82343.1	6.92	82470.3	43.17	3-8	Sunny	North	3-4

SV:Sampling volume, MC:Mass concentration, T:Temperature, W:Weather, WD:Wind direction, WS:Wind scale

and meteorological parameters are shown in Table 1. To collect the organic film, purified low-dust wiping paper stained with methylene chloride (Kimwipes, Kimberly Clark, USA) was used to wipe glass surfaces. The collected samples were wrapped in aluminum foil in a self-sealing bag. The complete collection process is described by Yu et al. [23]. In order to discuss the condensation and distribution process of PAHs between PM and organic film, samples of PM and organic film were collected simultaneously at each sampling site.

Sample Pretreatment and Instrument Analysis

The PAH extraction procedure used in this study was modified from the procedure described by Yu et al. [23]. The weighed samples (organic film/$PM_{2.5}$/PM_{10}), copper powder (3g), and anhydrous sodium sulfate (5g) were filled with deuterated internal standards (naphthalene-d_8, acenaphthene-d_{10}, phenanthrene-d_{10}, chrysene-$d_{12,}$ and perylene-d_{12}) in the filter paper tank (Dr. Ehrenstorfer GmbH, Germany). A 120 mL mixture of acetone and methylene chloride (volume ratio = 1:1) was prepared. Continuous reflux extraction was performed for 24 hours (4 times/hour) using a Soxhlet extractor. The extraction solution was rotated and evaporated to 1 mL, and the solvent was replaced with *n*-hexane. Impurities were removed using a silica-alumina chromatography column (volume ratio = 2:1, wet filling), and alkanes and aromatic hydrocarbon components were eluted using *n*-hexane (15 mL) and mixture solvent (70 mL; volume ratio of dichloromet hane and *n*-hexane = 3:7). The aromatic hydrocarbon components were evaporated to 1 mL for instrumental analysis.

Gas chromatography-mass spectrometry (GC-MS, Agilent, 7890A/5975C, Agilent Technologies Co. Ltd., USA) was used to detect 16 PAHs(naphthalene(Nap), acenaphthylene(Acy), acenaphthene(Ace), fluorene(Fluo), phenanthrene(Phe), anthracene (An), fluoranthene(Fl), pyrene(Pyr), benzo[a]anthracene(BaA), chrysene(Chry), benzo[b]fluor anthene(B[b]F), benzo[k] fluoranthene(B[k]F), benzo[a]pyrene(BaP), indeno[1,2,3-cd]pyrene (InP), dibenz[a,h]anthracene(DahA) and benzo[ghi]perylene(BghiP)) that are priority controlled by the USEPA. B[b]F and B[k]F were calculated together as B[b+k]F because their peaks could not be identified separately in the chromatographic analysis. The chromatographic column was a DB-5 polysiloxane polymer column (30 m × 0.25 mm × 0.25 μm). The temperature was held at 55ºC for 2 min to heat the instrument. The temperature was then increased at 20ºC/min to 280ºC, followed by 10ºC/min to 310ºC. The carrier gas consisted of high-purity helium; the flow rate was 1 mL/min, and SIM scanning was used.

Quality Assurance and Quality Control

Nap and Phe were detected in some field blank samples (less than 3% of the actual sample content). No PAHs were detected in the method blank, and the recovery rate of the 16 PAHs was 71.1-110%. The recovery rates of the deuterated internal standards *Nap-d_8*, *Ace-d_{10}*, *Phe-d_{10}*, *Chry-$d_{12,}$* *and* *Per-d_{12}* were 79.5-94.6%, 78.4-95.7%, 75.4-98.1%, 78.4-106.2%, and 79.5-101.6%, respectively.

Data Processing and Mapping

The mass concentration of PAHs on the glass surface is calculated as follows: Area - normalized mass concentration = C/A(The unit is ng/m^2, *C* is the average mass concentration of 2 samples per sampling site, and *A* is the sampling area). The Freehand and Originpro 2022 software were used to draw the graphs.

Table 2. Concentrations and ratios of atmospheric particulate matter (mg/m^3) and PAHs (ng/m^3).

Sampling site	$PM_{2.5}$	PM_{10}	Ratio	$PM_{2.5}$-bound PAHs	PM_{10}-bound PAHs	Ratio
ZSP	12.27	37.98	32.3%	12	12.4	96.8%
JT	9.79	47.92	20.4%	9.3	10.6	87.7%
SJUT	7.55	58.53	12.9%	7.6	9.8	77.6%
TQ	15.01	54.08	27.8%	14.8	18.5	80.0%
ZP	15.75	44.24	35.6%	25.5	26.7	95.5%
HN	12.53	49.58	25.3%	10.3	12.7	81.1%
SG	12.86	89.50	14.4%	3.5	3.6	97.2%
ECNU (H)	224.44	248.99	90.1%	16.6	16.8	98.8%
ECNU (NH)	6.92	43.17	16.0%	7.2	8.8	81.8%

Results and Discussion

Concentration Characteristics

As shown in Table 2, with the exception of ECNU(H), the mass concentration of $PM_{2.5}$ ranged from 6.92 to 15.75 mg/m^3, and the mass concentration of PM_{10} ranged from 37.98 to 89.50 mg/m^3. Among the sample sites, the $PM_{2.5}$ mass concentration was lowest at ECNU(NH) (6.92 mg/m^3) and highest at ZP (15.75 mg/m^3). The PM_{10} mass concentration was lowest at ZSP (37.98 mg/m^3) and highest at SG (89.50 mg/m^3). The SG samples were collected under foggy weather conditions. High humidity air increases the volume of aerosol particles, significantly reduces the visibility, and further aggravates the pollution. This cumulative effect of significantly increases the concentration of PM_{10}. The proportion of $PM_{2.5}/PM_{10}$ at each sampling point ranged from 12.9% to 35.6%, indicating that under good air quality conditions, 2.5-10 μm particles are the most abundant particle sizes in the atmosphere of Shanghai. In contrast, during haze weather, the mass concentration of $PM_{2.5}$ at ECNU(H) was 224.44 mg/m^3, while PM_{10} was 248.99 mg/m^3; the mass concentration ratio of $PM_{2.5}/PM_{10}$ was as high as 90.1%, indicating that during haze weather, the particulate matter in Shanghai's atmosphere is generally less than 2.5 μm.

Under good air quality conditions, the mass concentration of PAHs in $PM_{2.5}$ was 3.5-25.5 ng/m^3, and the mass concentration of PAHs in PM_{10} was 3.6-26.7 ng/m^3. The highest mass concentrations of PAHs in $PM_{2.5}$ and PM_{10} (25.5 ng/m^3 and 26.7 ng/m^3, respectively) were recorded at ZP, while the lowest mass concentrations were recorded at SG (3.5 ng/m^3 and 3.6 ng/m^3, respectively). The mass concentrations of PAHs in $PM_{2.5}$ and PM_{10} in haze weather were 16.6 ng/m^3 and 16.8 ng/m^3, respectively. The mass concentration ratio of PAHs in $PM_{2.5}$ and PM_{10} was as high as 77.6-98.8%, indicating that PAHs are more likely to adsorb on $PM_{2.5}$ than on PM_{10}, which is consistent with the studies of Wang et al. [22]. Environmental monitoring and management departments should pay special attention to $PM_{2.5}$ emissions because $PM_{2.5}$-bound PAHs easily enter the human respiratory system, including the lungs, causing substantial harm to the human body [1]. The normalized mass concentration of PAHs on glass surfaces was 85.9-592.9 ng/m^2. The highest concentrations were recorded at ECNU (592.9 ng/m^2) and ZP (343.8 ng/m^2); the lowest concentration was recorded at SG (85.9 ng/m^2). ECNU is located in Minhang District, close to the Wujing Town thermal power plant and the Huangpu River freight terminal. Emissions from coal-fired power plants and passing ships, the main sources of PAHs in the organic film, adsorb easily onto glass surfaces. In contrast, the SG sampling site is located in the undeveloped Nanhuizui area of Shanghai, where agricultural production is the main industry and where there is no large pollutant emission source. The mass concentration characteristics of specific monomeric PAHs are shown in Table 3 and Fig. 2.

Compositional Characteristics

PAHs are a class of semi-volatile organic compounds. Due to the small particle-gas distribution coefficient of low molecular weight PAHs, they are easily distributed in the gas phase and can condense and adsorb on glass surfaces. In contrast, high molecular weight PAHs have a larger particle-gas distribution coefficient and are more inclined to be distributed in PM. The compositional characteristics of $PM_{2.5}$- and PM_{10}-bound PAHs and organic film are shown in Fig.3. Except at sample site SG, the most abundant PAHs in $PM_{2.5}$ and PM_{10} are 4-ring PAHs ($PM_{2.5}$: 31.0%-44.4%, with an average of 40.5%; PM_{10}: 33.6%-46.1%, with an average of 41.8%), followed by 5- and 6-ring PAHs ($PM_{2.5}$: 31.2%-43.8%, with an average of 38.3%; PM_{10}: 31.9%-46.1%, with an average of 38.0%). The least abundant PAHs are 2- and 3-ring PAHs ($PM_{2.5}$: 12.6%-27.7%, with an average of 21.2%; PM_{10}: 12.4%-27.0%, with an average of 20.2%). The geographical location of SG differs from that of

Table 3. Concentrations of polycyclic aromatic hydrocarbons in atmospheric particulate matter (ng/m^3) and organic film (ng/m^2)

Sampling site	Environmental media	NaP	Acy	Ace	Fluo	Phe	An	Fl	Pyr	BaA	Chry	B[b+k]F	BaP	InP	DahA	B[ghi]P	T-PAHs
ZSP	$PM_{2.5}$	0.4	0.1	0.1	0.3	1.7	0.3	1.5	1.6	0.6	1.4	1.8	0.7	0.7	0.1	0.7	12.0
	PM_{10}	0.5	0.1	0.1	0.4	1.7	0.3	1.6	1.6	0.7	1.5	1.8	0.7	0.6	0.1	0.7	12.4
	Organic film	22.7	1.9	12.2	13.7	64.2	7.7	25.3	26.1	3.1	16.2	6.8	4.8	1.7	0.9	4.0	211.3
TQ	$PM_{2.5}$	0.4	0.1	0.1	0.4	1.5	0.2	2.0	1.8	0.6	1.9	2.8	0.8	0.9	0.2	1.1	14.8
	PM_{10}	0.5	0.1	0.1	0.4	1.9	0.2	2.6	2.2	0.8	2.4	3.5	1.0	1.2	0.2	1.4	18.5
	Organic film	24.8	1.9	23.2	13.5	65.0	6.7	19.4	21.7	3.7	17.7	8.5	9.3	2.0	1.1	4.3	222.8
ZP	$PM_{2.5}$	0.4	0.1	0.1	0.4	2.0	0.2	3.3	3.2	1.6	3.1	5.0	2.1	1.7	0.3	2.0	25.5
	PM_{10}	0.5	0.1	0.1	0.4	2.0	0.2	3.7	3.6	1.7	3.3	5.1	2.1	1.7	0.3	1.9	26.7
	Organic film	31.7	2.7	25.5	18.0	79.8	9.6	34.8	36.2	10.6	36.8	27.1	7.6	7.9	2.6	12.9	343.8
HN	$PM_{2.5}$	0.4	0.1	0.1	0.4	1.2	0.2	1.0	1.0	0.5	1.3	2.2	0.4	0.7	0.1	0.7	10.3
	PM_{10}	0.4	0.1	0.2	0.3	1.2	0.2	1.0	1.0	0.8	1.7	3.0	0.8	0.9	0.1	1.0	12.7
	Organic film	17.3	1.6	10.9	12.4	55.6	7.0	10.3	17.5	3.9	15.7	6.2	3.9	1.3	2.8	2.4	168.8
SG	$PM_{2.5}$	0.4	0.1	0.1	0.3	1.0	0.2	0.3	0.3	0.1	0.3	0.2	0.0	0.1	0.0	0.1	3.5
	PM_{10}	0.4	0.1	0.1	0.4	1.0	0.2	0.3	0.3	0.1	0.3	0.2	0.0	0.1	0.0	0.1	3.6
	Organic film	6.4	1.1	2.0	3.2	15.8	1.9	11.9	8.9	3.3	9.9	7.1	3.1	4.1	1.3	5.9	85.9
JT	$PM_{2.5}$	0.4	0.1	0.3	0.4	1.1	0.2	0.7	0.7	0.4	1.1	1.9	0.5	0.7	0.1	0.7	9.3
	PM_{10}	0.4	0.1	0.1	0.4	1.4	0.2	0.9	0.9	0.5	1.3	2.1	0.6	0.7	0.2	0.8	10.6
	Organic film	31.8	3.3	14.1	15.6	69.7	9.0	27.1	29.1	9.9	27.8	23.3	5.3	6.4	2.0	8.5	282.9
SJUT	$PM_{2.5}$	0.3	0.1	0.5	0.2	0.9	0.1	0.9	0.9	0.3	1.0	0.8	0.4	0.5	0.1	0.6	7.6
	PM_{10}	0.3	0.1	0.5	0.2	1.3	0.2	1.4	1.3	0.5	1.3	0.9	0.5	0.6	0.1	0.6	9.8
	Organic film	18.1	2.4	24.6	12.8	56.8	8.6	19.4	23.9	10.0	25.9	17.9	3.7	4.4	1.7	5.4	235.6
ECNU	$PM_{2.5}$(H)	0.2	0.1	0.3	0.2	1.2	0.2	2.0	1.9	1.0	2.5	2.2	1.4	1.5	0.3	1.6	16.6
	PM_{10}(H)	0.2	0.1	0.4	0.2	1.2	0.2	2.0	1.9	1.0	2.5	2.2	1.4	1.5	0.3	1.7	16.8
	$PM_{2.5}$(NH)	0.2	0.1	0.4	0.2	0.7	0.1	1.0	0.9	0.6	0.5	0.8	0.4	0.5	0.1	0.7	7.2
	PM_{10}(NH)	0.3	0.1	0.5	0.2	0.9	0.2	1.0	1.1	0.6	1.1	0.8	0.7	0.6	0.1	0.6	8.8
	Organic film	32.0	0.0	14.3	23.2	107.7	12.9	83.0	77.4	30.8	57.1	76.3	42.8	15.8	5.9	13.7	592.9

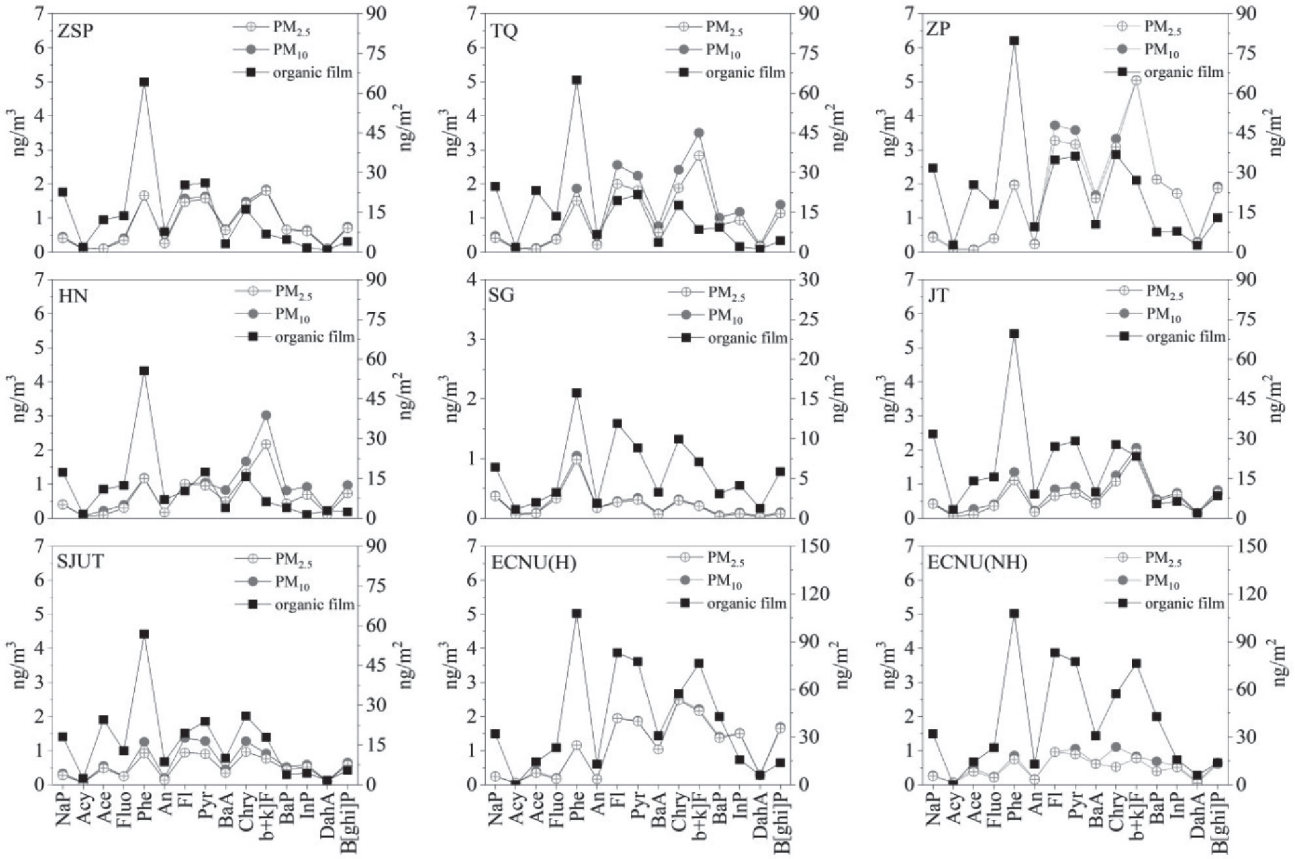

Fig. 2. Concentrations of polycyclic aromatic hydrocarbons in atmospheric particulate matter (ng/m^3) and organic film (ng/m^2).

the other sampling sites, and there are differences in the sources and types of pollutants. At SG, 2- and 3-ring PAHs are most abundant ($PM_{2.5}$: 60.5%, PM_{10}: 57.9%), followed by 4-ring PAHs ($PM_{2.5}$: 27.4%, PM_{10}: 28.8%). The 5- and 6-ring PAHs are least abundant ($PM_{2.5}$: 12.1%, PM_{10}: 13.3%). The most abundant PAHs in organic film are 2- and 3-ring PAHs (32.0%–62.1%, with an average of 49.9%), followed by 4-ring PAHs (28.0%-41.9%, with an average of 34.1%), and 5- and 6-ring PAHs (8.6%-26.1%, with an average of 16%). As shown in Fig. 3, the compositional characteristics of $PM_{2.5}$- and PM_{10}-bound PAHs at SG differ greatly

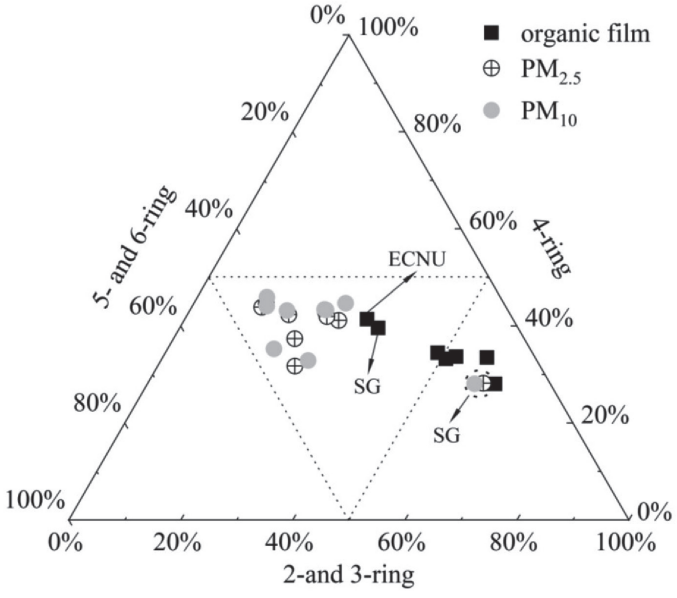

Fig.3 Compositional characteristics of PAHs in atmospheric particulate matter and organic film

from those at other sampling sites but are similar to the composition of PAHs in organic film. Further research on the composition of PAHs is needed.

Gas-Film Partitioning

Condensation and distribution processes control the migration and fate of organic pollutants in environmental media [24]. Mackay described the distribution processes of different soluble compounds between multiple interfaces and concluded that organic pollutants adsorb to glass surfaces through condensation to form an organic loading layer. The process of distribution between the air-organic film interface can then occur. Octanol, a substitute for the organic phase in the environment, can be used to describe the distribution characteristics of organic pollutants between organic film and the atmosphere via the octanol-air partition coefficient (K_{OA}). Harner tested the accuracy of K_{OA} and predicted the distribution characteristics of organic pollutants between the gas phase and the particle phase [25]. In addition, K_{OA} can be used to predict the distribution of organic pollutants between the gas-soil and gas-vegetation system interfaces [26].

The K_{OA} is calculated using the formula:

$$K_{OA} = C_O/C_A = K_{OW}/K_{AW},$$

where C_O is the concentration of octanol compounds, C_A is the concentration of pollutants in the atmosphere, K_{OW} is the octanol-water distribution coefficient, K_{AW} is the infinite air-water distribution coefficient equal to $H/(RT)$, H is the Henry constant, R is the ideal gas constant, and T is the absolute temperature.

The experimentally deduced organic film-air distribution coefficient (K_{FA}) is calculated using the formula:

$$K_{FA} = F_C(ng/m^3)/P_C(ng/m^3),$$

where F_C is the concentration of the organic film (unit area concentration/volume organic film thickness (Ft), Ft = $M(mg/m^2)\times10^9(nm/m)/1.7\times10^9$ (mg/m^3), M is area - normalized mass concentration, $1.7\times10^9(mg/m^3)$ is the density of aerosol.) and P_C is the geometric mean concentration of $PM_{2.5}$ and PM_{10}.

K_{FA} describes the balanced distribution of organic pollutants in organic film and the atmosphere; it is meaningful only in that the atmospheric-organic film balance is achieved because organic film is very thin in nature, allowing the rapid attainment of equilibrium [16]. Whether organic pollutants have reached an equilibrium between the organic film and the atmosphere can be assessed by comparing $\log K_{FA}$ and $\log K_{OA}$ [27]. In this study, the $\log K_{FA}$ (3% OM) and $\log K_{FA}$ (20% OM) of Nap, Acy, Ace, Fhe, Phe, An, Fl, Pyr, and Chry are more than one order of magnitude higher than the $\log K_{OA}$ in the literature (Table 4), which indicates that these monomer PAHs reach a dynamic equilibrium between the organic film and PM. These results also imply that when the concentration of PAHs in the urban atmosphere decreases over a period of time, the concentration in the organic film also decreases accordingly [28]. This process could also explain Gustafson and Dickhut's observation that PAHs can evaporate into the atmosphere from the surface of the contaminated impervious layer with increasing temperature [29].

Source Analysis

The composition of PAHs in the environmental medium varies due to different pollution sources [30,31]. Therefore, Fl/(Fl + Pyr), InP/(InP + BghP), BaP/BghP, and BaA/(BaA + Chry), which have relatively stable characteristics, are often used as indicators to determine PAH sources. Previous studies have shown that an InP/(InP + BghP) ratio between 0.2 and 0.5 indicates that oil combustion is the primary PAH source; a ratio greater than 0.5 indicates that coal, grass, and wood combustion are the sources. A Fl/(Fl + Pyr) ratio of less than 0.4 indicates that oil emission is the primary PAH source. When the ratio is between 0.4 and 0.5, liquid fuel combustion is the primary PAH source, and when it is greater than 0.5, biomass and coal combustion is the primary PAH source. A BaA/(BaA + Chry) ratio of less than 0.2 indicates that the PAH source is oil emissions. A ratio of between 0.2 and 0.35 indicates a mixed oil and liquid fuel combustion sources, and a ratio of greater than 0.35 indicates a biomass and coal combustion source. When the BaP/BghP ratio is less than 0.6, non-motor vehicle emissions are the primary PAH source; when it is greater than 0.6, vehicle emissions represent the primary PAH source. As shown in Fig.4, in this study, the ratio of InP/(InP + BghP) in organic film, $PM_{2.5}$, and PM_{10} is generally between 0.2 and 0.5, while the ratio of Fl/(Fl + Pyr) is generally between 0.4 and 0.5, indicating that the PAH source is related to the combustion of liquid fuels, including the combustion of petroleum substances such as diesel and gasoline. The ratio of BaA/(BaA + Chry) is mainly between 0.2 and 0.35, and the ratio of BaP/BghP is generally greater than 0.6, indicating that the PAHs are derived primarily from mixed petroleum and liquid fuel sources, especially motor vehicle emissions. In conclusion, the PAHs in the organic film, $PM_{2.5}$, and PM_{10} are derived from petroleum combustion, and the contribution of automobile exhaust is obvious.

Due to notable differences in environmental parameters in different study areas, the degradation rate of PAHs in the migration process may also differ; thus, there may be some errors in source determination results obtained by referring to the isomer ratio in other studies. In this study, the source component spectrum data of PAHs in Shanghai were used to determine PAH sources. As shown in Fig. 4, the InP/(InP + BghP) ratios of $PM_{2.5}$ and PM_{10} are relatively close to source component spectra 3, 5, 6, 7, and 8, which represent diesel vehicle

Table 4. Comparison of calculated K_{FA} with literature values of K_{OA}.

PAHs	ZSP		TQ		ZP		HN		SG		JT		SJUT		Reference
	$logK_{FA}$ (3% OM)	$logK_{FA}$ (20% OM)	$logK_{FA}$ (3% OM)	$logK_{FA}$ (20% OM)	$logK_{FA}$ (3% OM)	$logK_{FA}$ (20% OM)	$logK_{FA}$ (3% OM)	$logK_{FA}$ (20% OM)	$logK_{FA}$ (3% OM)	$logK_{FA}$ (20% OM)	$logK_{FA}$ (3% OM)	$logK_{FA}$ (20% OM)	$logK_{FA}$ (3% OM)	$logK_{FA}$ (20% OM)	$logK_{OA}$ [27]
NaP	10.0	10.9	10.1	11.0	10.6	11.4	9.8	10.6	9.5	10.3	10.1	10.9	9.9	10.7	6.2
Acy	9.0	9.8	9.0	9.9	9.5	10.3	8.7	9.6	8.7	9.5	9.1	9.9	9.0	9.8	6.3
Ace	9.8	10.6	10.1	10.9	10.5	11.3	9.6	10.4	9.0	9.8	9.8	10.6	10.0	10.8	-
Fluo	9.8	10.6	9.9	10.7	10.3	11.1	9.6	10.5	9.2	10.0	9.8	10.6	9.7	10.6	6.6
Phe	10.5	11.3	10.6	11.4	11.0	11.8	10.3	11.1	9.9	10.7	10.4	11.3	10.4	11.2	7.3
An	9.6	10.4	9.6	10.4	10.1	10.9	9.4	10.2	9.0	9.8	9.6	10.4	9.6	10.4	7.1
Fl	10.1	10.9	10.0	10.9	10.6	11.4	9.5	10.4	9.8	10.6	10.0	10.9	9.9	10.7	8.3
Pyr	10.1	10.9	10.1	10.9	10.6	11.5	9.8	10.6	9.6	10.4	10.1	10.9	10.0	10.8	-
BaA	9.2	10.0	9.3	10.1	10.1	10.9	9.1	9.9	9.2	10.0	9.6	10.4	9.6	10.5	9.1
Chry	9.9	10.7	10.0	10.8	10.6	11.5	9.7	10.6	9.7	10.5	10.0	10.9	10.0	10.9	9.4
B[b+k]F	9.5	10.3	9.7	10.5	10.5	11.3	9.3	10.2	9.5	10.4	10.0	10.8	9.9	10.7	10.7
BaP	9.4	10.2	9.7	10.5	10.0	10.8	9.1	10.0	9.2	10.0	9.3	10.2	9.2	10.0	10.9
InP	8.9	9.7	9.1	9.9	10.0	10.8	8.7	9.5	9.3	10.1	9.4	10.2	9.3	10.1	11.6
DahA	8.6	9.4	8.8	9.6	9.5	10.3	9.0	9.8	8.8	9.6	8.9	9.7	8.9	9.7	13.7
B[ghi]P	9.3	10.1	9.4	10.2	10.2	11.0	8.9	9.7	9.4	10.3	9.5	10.4	9.4	10.2	11.8

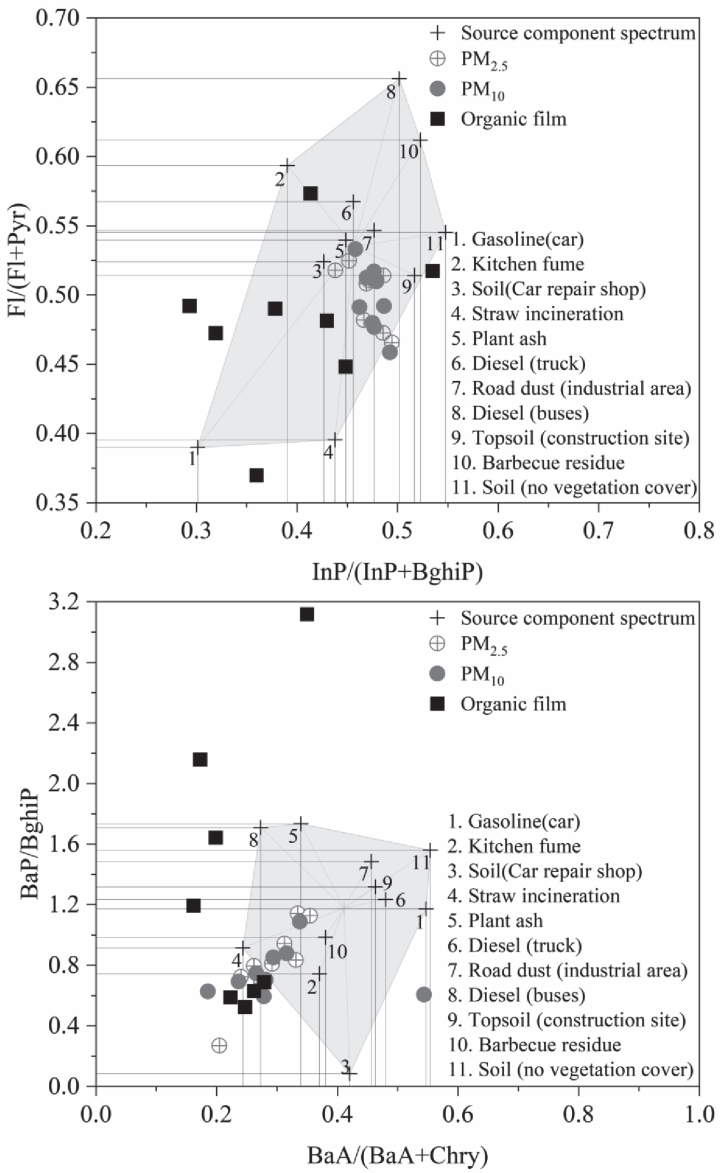

Fig. 4. Diagnostic coefficients of PAHs sources in atmospheric particulate matter and organic film.

exhaust (buses and trucks), plant ash, industrial road dust, and exposed garage topsoil. The ratios of Fl/(Fl + Pyr) are relatively close to spectra 3, 5, and 9, which represent exposed garage topsoil, plant ash, industrial road dust, and construction site topsoil. These ratios indicate that PAHs in Shanghai are mainly generated from automobile exhaust and dust sources. The BaA/(BaA + Chry) ratios are close to those of 4, 5, and 8, which represent the compositions of plant ash, burning straw, and diesel vehicle exhaust (buses); the BaP/BghP ratio is close to 2, 4, 6 and 10, which represent the compositions of kitchen lampblack, plant ash, barbecue residues, and diesel vehicle exhaust (trucks). These results indicate that diesel vehicle exhaust, domestic emissions (kitchen lampblack and barbecue residues), and field straw and vegetation incineration contribute greatly to PAHs. The above analysis shows that PAHs in $PM_{2.5}$ and PM_{10} primarily come from automobile exhaust (diesel vehicles), fugitive dust (road dust, bare surface, and vegetation/straw burning) and domestic emissions (kitchen lampblack and barbecue residues). The isomer ratio of PAHs in organic film is dispersed, and there is a significant difference compared to PM. It is possible that a strong photodegradation process occurs on the glass surface but not on the other media. The degradation rate of some monomer PAHs in organic film (such as BaA) is relatively fast. The source analysis of PAHs in organic film should be further studied using other methods..

Conclusions

In this study, we measured the mass concentration of PAHs in $PM_{2.5}$, PM_{10}, and organic film. The results show that the mass concentrations, compositional characteristics, and PAH sources in $PM_{2.5}$, PM_{10}, and

organic film vary substantially in different sampling areas. Under normal weather conditions, 2.5-10 μm particles are particularly abundant in the atmosphere of Shanghai; during haze periods, less than or equal to 2.5 μm particles are more abundant. Organic film tends to adsorb 2- and 3-ring PAHs, while $PM_{2.5}$ and PM_{10} are more enriched in 4-ring PAHs. Nap, Acy, Ace, Fluo, Phe, An, Fl, Pyr, and Chry quickly reach a dynamic equilibrium between the organic film and the atmosphere but rapidly adjust when the environment (e.g., temperature and light) changes. PAHs in $PM_{2.5}$, PM_{10}, and organic film are derived primarily from automobile exhaust, ground dust, and domestic emission sources; however, due to strong photodegradation on glass surfaces, source analyses of PAHs in organic film need to be studied more comprehensively.

Acknowledgments

This work was supported by grants from the National Natural Science Foundation of China (Grant Nos. 41730646, 42230505), the Natural Science Foundation of the Jiangsu Higher Education Institutions of China (Grant Nos. 20KJB170030), Wuxi Philosophy and social science bidding project (Grant Nos. WXSK23-C-136), Wuxi Soft Science Research Project (Grant Nos. KX-23-C018).

Conflict of Interest

There is no conflict of interest between authors.

References

1. TIAN Y.Z., JIA B., ZHAO P., SONG D.L., HUANG F.X., FENG Y.C. Size distribution, meteorological influence and uncertainty for source-specific risks: $PM_{2.5}$ and PM_{10}-bound PAHs and heavy metals in a Chinese megacity during 2011-2021. Environmental Pollution **312**, 120004, **2022**.
2. WHO, WHO global air quality guidelines: particulate matter($PM_{2.5}$ and PM_{10}), ozone, nitrogen dioxide, sulfur dioxide and carbon monoxide. **2021**.
3. MARKOZANNES G., PANTAVOU K., RIZOS E.C., SINDOSI O.A., TAGKAS C., SEYFRIED M., SALDANHA I.J., HATZIANASTASSIOU N., NIKOLOPOULOS G.K., NTZANI E. Outdoor air quality and human health: an overview of reviews of observational studies. Environmental Pollution **306**, 119309, **2022**.
4. WU F.H., CHI Y., ZHOU F. Spatio-temporal distribution of particulate matter(PM_{10} and $PM_{2.5}$) concentrations in urban subway station-a case of Nanning in China. Polish Journal of Environmental Studies **31**, 5895, **2022**.
5. WORLD BANK. The global health cost of $PM_{2.5}$ air pollution: a case for action beyond 2021. World Bank Publications: Washington, DC, USA. **2022**.
6. ZHANG X.L., YANG Z. The influence of technological innovation on $PM_{2.5}$ concentration in the Yangtze River Delta, China. Polish Journal of Environmental Studies **32**, 3915, **2023**.
7. YU Y.J., WANG Q., LI L.Z., SUN P., ZHANG Y.P., LIN H.P., CHEN J.H., LIN B.G., XIANG M.D. The variations of concentrations, profiles and possible sources of metals and polycyclic aromatic hydrocarbons in PM_{10} from Lanzhou, China. Polish Journal of Environmental Studies **25**, 1323, **2016**.
8. ZHEN Z.X., YIN Y., CHEN K., ZHEN X.L., ZHANG X., JIANG H., WANG H.L., KUANG X., CUI Y., DAI M.M., HE C.A., LIU A.K., ZHOU F.H. Concentration and atmospheric transport of $PM_{2.5}$-bound polycyclic aromatic hydrocarbons at Mount Tai, China. Science of the Total Environment **786**, 147513, **2021**.
9. SZEWCZYŃSKA M., DĄBROWSKA J., PYRZYŃSKA K. Polycyclic aromatic hydrocarbons in the particles emitted from the diesel and gasoline engines. Polish Journal of Environmental Studies **26**, 801, **2017**.
10. ZHANG X., ETO Y., AIKAWA M. Risk assessment and management of $PM_{2.5}$-bound heavy metals in the urban area of Kitakyushu, Japan. Science of the Total Environment **795**, 148748, **2021**.
11. JIA B., TIAN Y.Z., DAI Y.Q., CHEN R., ZHAO P., CHU J.J., FENG X., FENG Y.C. Seasonal variation of dissolved bioaccessibility for potentially toxic elements in sizeresolved PM: impacts of bioaccessibility on inhalable risk and uncertainty. Environmental Pollution **307**, 119551, **2022**.
12. BESIS A., GALLOU D., AVGENIKOU A., SERAFEIM E., SAMARA C. Size-dependent in vitro inhalation bioaccessibility of PAHs and O/N PAHs-Implications to inhalation risk assessment. Environmental Pollution **301**, 119045, **2022**.
13. FANG B., ZENG H., ZHANG L., WANG H.W., LIU J.J., HAO K.L., ZHENG G.Y., WANG M.M., WANG Q., YANG W.Q. Toxic metals in outdoor/indoor airborne $PM_{2.5}$ in port city of Northern, China: characteristics, sources, and personal exposure risk assessment. Environmental Pollution **279**, 116937, **2021**.
14. KONG F., WANG Y.F., FANG J., LU L.L. Spatial pattern of summer extreme precipitation and its response to urbanization in China(1961-2010). Resources and Environment in the Yangtze Basin **27**, 996, **2018**.
15. LIU J.H., LUO Z.R., ZHANG Y.X., ZHOU J.J., SHAO W.W. Influence of urbanization on spatial distribution of extreme precipitation in Henan Province. Water Resources Protection **38**, 100, **2022**.
16. DIAMOND M.L., GINGRICH S.E., FERTUCK K., MCCARRY B.E., STERN G.A., BILLECK B., GRIFT B., BROOKER D., YAGER T.D. Evidence for organic film on an impervious urban surface: Characterization and potential teratogenic effects. Environmental Science and Technology **34**, 2900, **2000**.
17. GINGRICH S E. Atmospherically derived organic films on impervious surfaces: detection and characterization. Toronto: University of Toronto **1999**.
18. BI C.Y., LIANG Y.R., XU Y. Fate and transport of phthalates in indoor environments and the influence of temperature: a case study in a test house. Environmental Science and Technology **49**, 9674, **2015**.
19. CSISZAR S.A., DIAMOND M.L., THIBODEAUX L.J. Modeling urban films using a dynamic multimedia fugacity model. Chemosphere **87**, 1024, **2012**.
20. GOUIN T., THOMAS G.O., COUSINS I., BARBER J., MACKAY D., JONES K.C. Air-surface exchange of polybrominated diphenyl ethers and polychlorinated

biphenyls. Environmental Science and Technology **36**, 1426, **2002**.
21. Ministry of ecology and environment of the People's Republic of China. The State of China's Ecological Environment Bulletin **2022**.
22. WANG Q., LIU M., YU Y.P., LI Y. Characterization and source apportionment of $PM_{2.5}$-bound polycyclic aromatic hydrocarbons from Shanghai city, China. Environmental Pollution **218**, 118, **2016**.
23. YU Y.P., YANG Y., LIU M., ZHENG X., LIU Y., WANG Q., LIU W.Y. PAHs in organic film on glass window surfaces from central Shanghai, China: distribution, sources and risk assessment. Environmental Geochemistry and Health **36**, 665, **2014**.
24. MACKAY D. Multimedia environmental models: the fugacity approach. Lewis Publishers: Chlelsea, USA **1991**.
25. HARNER T., MACKAY D., JONES K.C. Model of the long-term exchange of PCBs between soil and the atmosphere in the Southern UK. Environmental Science and Technology **29**, 1200, **1995**.
26. MACKAY D., WANIA F. Transport of contaminants to the Aretic: partitioning, processes and models. The Science of the Total Environment **25**, 160-161, **1995**.
27. LAW N.L., DIAMOND M.L. The role of organic films and the effect on hydrophobic organic compounds in urban areas: an hypothesis. Chemosphere **36**, 2607, **1998**.
28. HORNBUCKLE K.C., EISENREICH S.J. Dynamics of gaseous semivolatile organic compounds in a terrestrial ecosystem-effects of diurnal and seasonal climate variations. Atmospheric Environment **30**, 3935, **1996**.
29. GUSTAFSON K.E, DICKHUT R.M. Particle/gas concentrations and distributions of PAHs in the atmosphere of Southern Chesapeake Bay. Environmental Science and Technology **31**, 140, **1997**.
30. YUNKER M.B., SNOWDON L.R., MACDONALD R.W., SMITH J.N., FOWLER M.G., SKIBO D.N., MCLAUGHLIN F.A., DANYUSHEVSKAYA A.I., PETROVA V.I., IVANOV G.I. Polycyclic aromatic hydrocarbon composition and potential sources for sediment samples from the Beaufort and Barents Seas. Environmental Science and Technology **30**, 1310, **1996**.
31. YIN H., XU L. Comparative study of PM_{10}/$PM_{2.5}$-bound PAHs in downtown Beijing, China: concentrations, sources, and health risks. Journal of Cleaner Production **177**, 674, **2018**.